Dynamic Mechanical Relaxations in Poly(acrylonitrile) with Different Stereoregularities

Daisuke Sawai and Tetsuo Kanamoto*

Department of Applied Chemistry, Tokyo University of Science, Kagurazaka, Shinjuku-ku, Tokyo 162-8601, Japan

Hitoshi Yamazaki and Kunio Hisatani

Fundamental Research Laboratory of Fibers and Fiber-Forming Polymers, Asahi Chemical Industry Co. Ltd., 11-7 Hacchonawate, Takatuki, Osaka 569, Japan

Received August 20, 2003; Revised Manuscript Received February 7, 2004

ABSTRACT: The dynamic mechanical properties of poly(acrylonitrile)s (PANs) with NMR triad isotacticities ranging from 0.25 to 0.68 and drawn to a draw ratio (DR) of 1−60 were measured at 0.5−110 Hz in the temperature range of −150 to 200 °C to study the effects of stereoregularity and DR on the relaxation behavior in PAN. Four kinds of relaxations were observed: α and α_c relaxations at around 150 °C, a β_c relaxation at around 100 °C, and a γ one at around 25 °C were observed as tan δ peaks measured at 3.5 Hz depending on the stereoregularity and DR. The magnitudes of the loss modulus E'' and tan δ peaks were sensitive to the isotacticity, DR, and thermal history of the samples. These results confirm the previous assignments of the α and β_c relaxations in at-PAN to the molecular motions in amorphous and paracrystalline phases, respectively, and they are also applicable to both iso- and at-PANs. Furthermore, the observed effects of the stereoregularity and DR on the relaxation behavior, crystallinity, and chain conformations studied by wide-angle X-ray diffraction suggested more details about the origins of these relaxations. The β_c and γ relaxations are predominantly ascribed to the segmental motions of helical sequences and planar zigzag sequences, respectively, both in paracrystalline phases. The lower tail of the loss peak due to the γ relaxation is likely ascribed to the local mode motions of conformationally disordered sequences. It is noted, however, that an ultradrawn at-PAN fiber with a DR of 60 exhibited a sharp tan δ peak at around 150 °C (α_c relaxation) that was associated with a sudden decrease in the storage modulus E' and a DSC endothermic peak. Therefore, both the molecular motion in amorphous regions of PANs (α relaxation) and that associated with the first-order thermal transition in paracrystalline phases of an ultradrawn at-PAN fiber (α_c relaxation) contribute to the relaxation at around 150 °C.

Introduction

Poly(acrylonitrile) (PAN) is an unusual polymer in that even atactic PAN (at-PAN) can crystallize. Although many articles have been published on the crystal structure,[1−7] phase structure,[3,8,9] chain conformation,[10−12] and molecular dynamics of at-PAN fibers,[13−23] ambiguities still remain, primarily due to the insufficient information about their chain conformation and morphologies. Wide-angle X-ray diffraction (WAXD) patterns of at-PAN fibers generally show only two or three discrete reflections on the equator and a few diffuse scatterings on the meridian and diagonals, revealing that the configurationally disordered chains generate significant disorder in the crystals. Most recent articles[11,23−25] have reported that this polymer takes a hexagonal or orthorhombic chain packing with no order along the chain axis (paracrystal).[14,26]

Another reason that ambiguities still remain is related to the fact that at-PAN shows no melting in bulk,[27] and it was difficult to prepare wide varieties of morphologies that might allow the correlation of each of the properties to its specific morphological origin. Furthermore, the fact that some of the fibers previously used were copolymers of acrylonitrile containing a small percentage of comonomers[13,18,22] or had heterotactic linkages such as chain branching[19] might also lead to the confusion.

The relaxations and/or thermal transitions in PAN have also been extensively studied by several techniques, including dynamic mechanical analyses (DMA),[15,17−19,21,23,28] dielectric measurements,[16,20] infrared absorption spectroscopy,[29] and WAXD at elevated temperatures[14,22,24,30] as summarized in Table 1. Some articles have reported only the β_c relaxation at around 85−110 °C.[13,14,16,20] Others observed one more relaxation (α relaxation) at 140−160 °C[15,17−19,21−23] in addition to the β_c relaxation. Commonly, the relaxations at lower and higher temperatures have been assigned to the molecular motions in paracrystalline phases and in amorphous regions (glass transition), respectively. The relaxation at around room temperature (γ relaxation) has seldom been mentioned. Our recent studies on ultradrawn at-PAN revealed the existence of a first-order crystal/crystal transition (α_c relaxation) at around 150 °C.[24,28] This thermally reversible transition was observed only in ultradrawn fibers. No further details of the effects of stereoregularity and DR on these relaxations and/or thermal transitions in PAN have been reported.

Recently, Rizzo et al.,[11] Hu et al.,[31] and Liu et al.[3] predicted that isotactic PAN (iso-PAN) takes a 3_1 helical chain conformation whereas syndiotactic PAN prefers a planar zigzag conformation, as shown by computer simulations. To our knowledge, the only available information on the effect of stereoregularity on the relaxations in PAN has been reported by Joh.[19] He reported only α relaxation in iso-PAN at around 150 °C

* To whom correspondence should be addressed.

10.1021/ma0352330 CCC: $27.50
Published on Web 03/16/2004

Table 1. Relaxation Temperatures for PAN Previously Reported by Several Researchers

authors	methods	draw ratio[a]	annealing temp (°C)	polymer type[b]	α (°C)[d]	β_c (°C)[d]	γ (°C)[d]	freq (Hz)
Howard[13]	expansion	1		at-homo, co		87(g)[e]		
Bohn et al.[14]	WAXD	4−9		at-homo		87(c)[f]		
Andrews et al.[15]	DMA	1		at-homo	140(g)	87(g)		
Hayakawa et al.[16]	dielectric	1	90−130	(co)		85(c)		10^0−10^6
Okajima et al.[17]	DMA	4−16	108	at-homo	160(c)	109(g)	80(?)	3.5−110
Minami et al.[18]	DMA	1−7	130	at-homo, co	160(g)	110(c)		110
Joh[19]	DMA	1	180	iso-homo[c]	160(g)	110(c)		110
Gupta et al.[20]	dielectric	1	-	at-homo		110(g)		10^2−10^5
Cho et al.[21]	DMA	1−8	120−160	at-homo	144(g)	103(c)		1−100
Rizzo et al.[22]	DMA, WAXD	2−14	140	at-homo, co	140(g)	100(c)		10
Bashir et al.[23]	DMA	1−10		at-homo	140(g)	90(c)	25(?)	1
our previous works[28,29]	DMA, WAXD, DSC	1		at-PAN	157(g)	104(c)		3.5
		50−150		at-PAN	150(c/c)[g]	98(c)	25(c)	3.5

[a] Draw ratio of 1 corresponds to an undrawn sample. [b] Homo = homopolymer; co = copolymer. [c] Isotactic and amorphous PAN with chain branching. [d] Relaxation temperature. [e] (g) = relaxation associated with the glass transition in amorphous regions. [f] (c) = relaxation associated with the molecular motion in crystalline regions. [g] (c/c) = crystal/crystal thermal transition.

Table 2. Characteristics of iso- and at-PAN Samples

		triad tacticity			gel film		EDR = 16			DR_t = 60		
sample	M_v	*mm*	*mr*	*rr*	E^a (GPa)	density (g/cm^3)	E (GPa)	f_c[b]	density (g/cm^3)	E (GPa)	f_c	density (g/cm^3)
iso-PAN-1	1.4×10^6	0.48	0.36	0.16	1.9	1.125	19.8	0.961	1.189	28.2	0.995	1.190
iso-PAN-2	3.5×10^6	0.58	0.29	0.13	2.4	1.109	20.5	0.963	1.189	31.5	0.996	1.192
iso-PAN-3	5.2×10^5	0.68	0.22	0.10	1.8	1.123	20.6	0.970	1.183	28.5	0.995	1.184
at-PAN	2.3×10^6	0.25	0.51	0.24	2.1	1.152	16.4	0.972	1.166	23.7	0.996	1.173

[a] Tensile modulus at room temperature. [b] Crystalline chain orientation function.

at 110 Hz, which was ascribed to the micro-Brownian motion in amorphous regions. However, it is important to remark that the WAXD patterns of his PAN recorded before and after annealing at 160 °C revealed that the PAN was amorphous. Although no detailed information on the microstructure was provided, he assumed that the amorphousness of his PAN was probably due to the multiple branchings of chains.

Recently, a series of well-characterized isotactic PANs with a ^{13}C NMR isotactic triad (*mm*) fraction of 0.25−0.68[25,30] became available to us. Furthermore, we have shown that both at- and iso-PAN's of high molecular weights could be ultradrawn to draw ratios (DR) over 50 by a two-stage drawing under controlled conditions.[24,25,30] Such highly drawn PAN fibers exhibited extreme structure and properties including a high crystalline chain orientation function, f_c, of 0.996−0.997 and high moduli of 28−32 GPa approaching the uncertain X-ray crystal modulus of at-PAN.[32]

The availability of well-characterized PANs with different stereoregularities and their draw ratio series including an ultradrawn morphology for both at- and iso-PANs stimulated us to study the effects of these variables on the relaxation behavior of PAN. In this paper, thus, we discuss the effects of stereoregularity (and hence chain conformation) and draw ratio (and hence morphology and conformation) on the dynamic mechanical properties for a series of PAN fibers with different isotacticities to improve our understanding of the complex relaxation characteristics of PAN.

Experimental Section

Samples. The four PANs used were homopolymers and had different isotactic triad fractions, *mm* = 0.25, 0.48, 0.58, and 0.68, as determined by ^{13}C NMR.[33] At-PAN (*mm* = 0.25) was prepared by suspension polymerization of acrylonitrile (AN). Iso-PAN-1 (*mm* = 0.48) and iso-PAN-2 (*mm* = 0.58) were prepared by polymerization of AN with organometallic compounds. Iso-PAN-3, having the highest isotacticity (*mm* = 0.68), was synthesized by γ-irradiation polymerization of AN within a urea canal complex at Asahi Chemical Co. Ltd.

The viscosity-average molecular weights (M_v) of PAN samples with different stereoregularities were calculated by the Mark−Houwink equation $[\eta] = K_m M_v^{\alpha}$, where the limiting viscosity number $[\eta]$ of PAN was measured in DMSO at 25 °C. The values of constants K_m and α for PANs with different stereoregularities were previously determined by Kamide et al.[34] and Nakano.[35] Briefly, they determined the parameters K_m and α for sharp molecular weight fractions of PAN prepared using radical initiators and fractions of PAN synthesized by γ-irradiation polymerization of AN within a urea canal complex as follows:

$$K_m = 0.153 \text{ and } \alpha = 0.60 \text{ for PAN with } mm = 0.27 \quad (mmmm = 0.077)$$

$$K_m = 0.204 \text{ and } \alpha = 0.58 \text{ for PAN with } mm = 0.52 \quad (mmmm = 0.39)$$

In the calculations of M_v, we estimated the parameters of K_m and α for PAN with triad isotacticities ranging from 0.25 to 0.68, assuming that they vary linearly with the triad isotacticity. The characteristics of these PANs are summarized in Table 2.

Polymer solutions with concentrations of 2 or 5 wt % were prepared by dissolving PAN in *N*,*N*′-dimethylformamide at 100 °C. The hot solutions were then transferred into stainless steel trays and quenched at 0 °C for 2 h to make gel. The wet gel films were extracted with methanol and then dried at room temperature in vacuo to constant weights.

Drawing. A two-stage draw technique was used to achieve a high DR.[24,25,30] The first-stage draw was made by solid-state coextrusion through a conical brass die at 125 °C and an extrusion draw ratio (EDR) of 16. The coextruded films were further drawn by a tensile force at constant temperatures of 100−200 °C in an air oven equipped with an Orientec Tensilon tensile tester RTC-1210 at constant cross-head speeds. The total draw ratio (DR_t), after the two-stage draw, is defined by DR_t = (first-stage EDR) × (second-stage DR).

Measurements. DMA measurements were made on an Orientec Rheovibron DDV-II-EP viscoelastometer operated at

frequencies of 3.5, 11, 35, and 110 Hz in the temperature range of −150 to 200 °C. The effects of stereoregularity and DR on the variations of the dynamic storage modulus (E'), loss modulus (E''), and loss tangent (tan δ) with temperature were measured at the lowest frequency of 3.5 Hz. The activation energies for the γ and β_c relaxations observed as the tan δ peaks at ∼25 and ∼100 °C, respectively, could be determined from the measurements on the viscoelastometer operated at frequencies of 3.5, 11, 35, and 110 Hz. However, the tan δ peak at around 150 °C due to the α relaxation, which was observed only in the as-prepared gels and at the lowest frequency of 3.5 Hz, merged into the strong β_c peak at around 100 °C for the measurements at higher frequencies. To determine the activation energy of this α relaxation, therefore, the tan δ peak was measured at lower frequencies of 0.5, 1, 4.9, and 9.8 Hz on a Toyo Seiki Rheolograph Solid operated at a heating rate of 1 °C/min.

Wide-angle X-ray diffraction (WAXD) profiles of drawn films were recorded with Ni-filtered Cu Kα radiation generated at 40 kV and 150 mA on a Rigaku Rotaflex RU-200 rotating anode X-ray generator equipped with a diffractometer. High resolution was necessary to detail the diffraction patterns at around $2\theta = 17°$ on the equator. The intensity was collected by step scans at 0.02° intervals in 2θ. The reflection profiles were measured by a symmetrical transmission mode. Line collimators of 0.05 mm (first), 0.15 mm (second), and 0.15 mm (third) were used for the measurements.

Differential scanning calorimetry (DSC) measurements were performed on a Seiko Denshi DSC-220C differential scanning calorimeter at a heating rate of 10 °C/min under a N_2 gas flow. The sample size for the measurements was 0.5−2 mg. The transition temperature and heat of transition were calibrated using an indium standard. The densities of samples were measured at 30 ± 0.1 °C in a density gradient column consisted of mixtures of *n*-heptane and carbon tetrachloride.

Results and Discussion

Structure of PAN Fibers. Before the discussion on the relaxation behavior of at- and iso-PAN's, the structures of PAN fibers used in this work were characterized. Figure 1 shows WAXD photographs of ultradrawn at-PAN and iso-PAN-3 fibers with a DR_t of 60. This iso-PAN-3 had the highest isotactic triad fraction of 0.68 among those used in this work. Independently of the stereoregularity, the WAXD photographs showed only two or three sharp reflections on the equator and diffuse and weak scatterings on the diagonal and meridian. This indicates that these PAN fibers had a paracrystalline structure in which the chains packed regularly, but there was no order along the chain axis.

The effect of stereoregularity was reflected on the strong equatorial scattering at around $2\theta = 17°$. Figure 2 shows the equatorial reflections at around $2\theta = 17°$ for a series of ultradrawn fibers with a DR_t of 60 and an isotactic triad fraction ranging from $mm = 0.25$ to 0.68. The at-PAN ($mm = 0.25$) showed two peaks corresponding to the (200) and (110) reflections of an orthorhombic chain packing with unit cell constants of $a = 1.03$ and $b = 0.61$ nm.[25] In contrast, all three iso-PANs with $mm = 0.48$−0.68 exhibited a single sharp peak corresponding to the (120, 200) reflection of an orthorhombic chain packing with $a = 1.03$ and $b = 1.22$ nm.[30,35] These results confirm that the highly drawn PAN fibers used in this work had a paracrystalline structure in which the chains are packed regularly with no order along the chain axis independently of the stereoregularity.

The WAXD studies showed that both at- and iso-PAN chains are arranged in an orthorhombic array[24,36] with no order along the chain axis independently of the stereoregularities. However, the chain conformation in

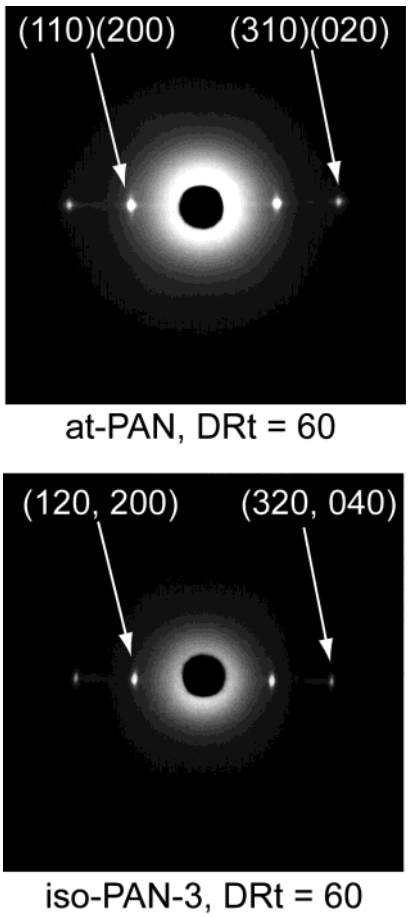

Figure 1. WAXD photographs of ultradrawn at- and iso-PAN-3 fibers with a DR_t of 60. Note that the breadths of the equatorial reflections are significantly broader in at-PAN than in iso-PAN-3.

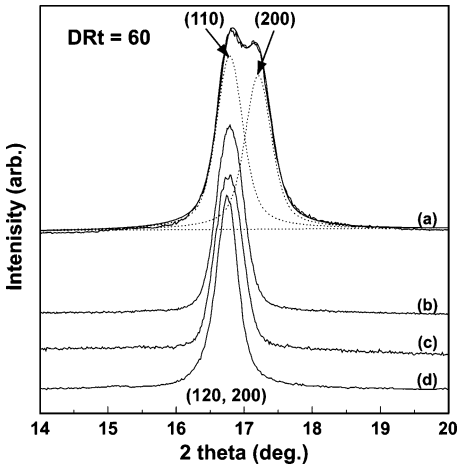

Figure 2. WAXD equatorial scans at around $2\theta = 17°$ for ultradrawn at-PAN (a), iso-PAN-1 (b), iso-PAN-2 (c), and iso-PAN-3 (d) fibers with a DR_t of 60.

paracrystalline phases is significantly affected by the stereoregularity of PANs. Hu et al.[31] and Rizzo et al.[11] have shown that the X-ray meridional scatterings of PAN fibers are related to the chain conformation of PAN crystals. Figure 3 shows WAXD diffractometer scans along the meridian in the 2θ range of 30°−45° (Cu Kα) for ultradrawn at- and iso-PAN fibers with a $DR_t = 60$. The scattering pattern of the at-PAN fiber shows a fairly strong peak at $2\theta \cong 36.3°$ and a weak one at $2\theta \cong 40°$, which corresponds to the *d*-spacings of ∼0.25 and ∼0.23

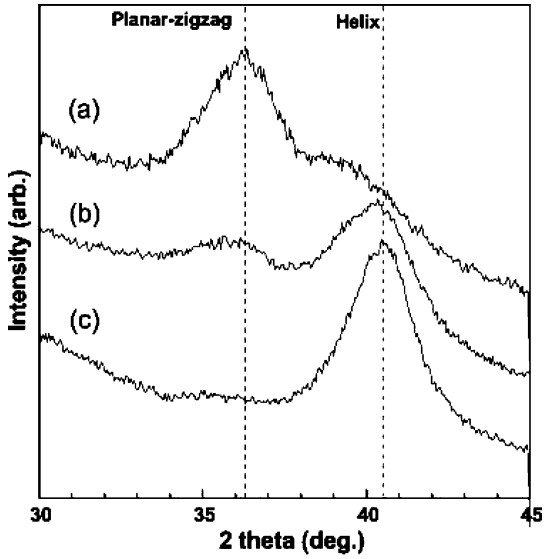

Figure 3. WAXD meridional scans at around $2\theta = 40°$ for ultradrawn at-PAN (a), iso-PAN-1 (b), and iso-PAN-3 (c) fibers with a DR_t of 60. Note that the peaks at $2\theta = 36.3°$ and ~40° are ascribed to the scatterings from planar zigzag and helical sequences, respectively.

nm, respectively. The 2θ value at higher angle was determined by the curve fitting. According to the model calculations combined with the observed WAXD patterns,[3,7,11,31] these scattering peaks were assigned to scatterings from the planar zigzag (syndiotactic and short isotactic) sequences and the 3_1 helical (long isotactic) ones, respectively. Consistent with these predictions, the intensity of the meridional scattering at around $2\theta \cong 40°$ assigned to the helical sequences increased whereas that around $2\theta \cong 36°$ ascribed to the planar zigzag sequences decreased with an increasing isotactic fraction, as seen in Figure 3. Thus, the iso-PAN-3 fiber having a *mm* of 0.68 mainly consisted of helical sequences with a small amount of planar zigzag sequences (Figure 3).

The structure and properties of PAN fibers were also affected by the sample DR_t. Upon drawing of the gel films, the crystalline chain orientation function (f_c), sample density, and tensile modulus (Table 2) increased rapidly with the DR_t and approached constant values at higher $DR_t > 30-100$ for both at- and iso-PANs, as discussed previously.[24,25,30] The ultradrawn PAN fibers used in this work exhibited an extreme f_c of 0.995−0.996 and a tensile modulus of 23.7−31.5 GPa approaching the still uncertain crystal modulus of PAN,[32] as shown in Table 2. These facts suggest that the morphology of as-prepared gel films can be expressed by an amorphous and crystalline two-phase structure, whereas that of highly drawn fibers is better approximated by a single-phase paracrystalline structure independently of the stereoregularity of PANs. Furthermore, upon drawing of at-PAN, the amount of planar zigzag sequences significantly increased with increasing DR_t, and an ultradrawn at-PAN fiber with a DR_t of 60 predominantly consisted of planar zigzag sequences although a significant amount of helical sequences was still present. Such an ultradrawn at-PAN fiber exhibited a crystal/crystal reversible transition at around 145 °C, as determined by DSC and WAXD at elevated temperatures.[24,28]

To examine the effect of stereoregularity on the thermal transition, DSC measurements were made for a series of ultradrawn PANs with a DR_t of 60 and are

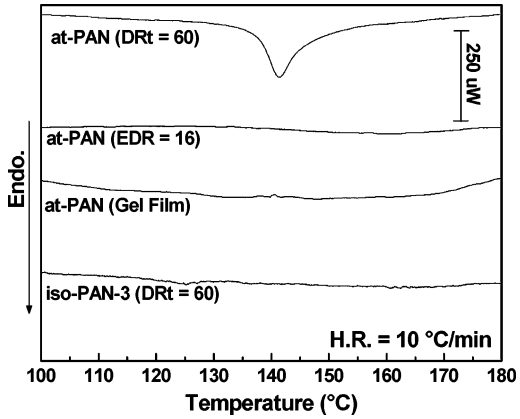

Figure 4. DSC thermograms for ultradrawn at-PAN and iso-PAN-3 fibers with a DR_t of 60. The thermograms of at-PAN fibers with lower DRs were also included to show the effect of DR.

shown in Figure 4. The thermograms for an at-PAN gel film and a fiber with a lower EDR of 16 are also included to show the effect of DR_t. A fairly sharp endothermic peak was observed at 142 °C only for the highly drawn at-PAN fiber, and no such transition was observed in the highly drawn iso-PAN fibers and the at-PAN samples with lower DR_t's.

Effect of Stereoregularity on the Relaxations. Gel films of PAN exhibited similar relaxation behavior independently of their stereoregularities. However, the effect of stereoregularity became significant upon drawing of these gel films. Figure 5 shows the effect of isotacticity on the temperature dependences of the E', E'', and tan δ for at-PAN, iso-PAN-1, and iso-PAN-3 fibers with an EDR of 16 measured at 3.5 Hz in the temperature range of −150 to 200 °C. At a low temperature, the E' was comparable for all samples and decreased slowly with the temperature up to ~50 °C. Above this temperature, the E' decreased rapidly with the temperature, suggesting the onset of large-scale segmental motion. This decrease in E' is slightly more rapid for the iso-PANs than for the at-PAN. A tan δ peak at 100 °C (β_c relaxation), corresponding to an E'' peak at around 85 °C, was observed in all of the PAN samples. However, the shape and magnitude of these peaks were sensitive to the isotacticity of PANs. The tan δ peak as well as the E'' peak became sharper and stronger with increasing isotacticity of the samples, suggesting that this loss peak is primarily associated with the molecular motion of isotactic sequences and, hence, with the helical sequences of PAN chains as discussed above based on the WAXD meridional scatterings (Figure 3). This β_c relaxation, which was associated with a significant decrease in the E', is ascribed to the molecular motion in paracrystalline phases as will be discussed later based on the effect of draw ratio on the relaxation behavior (Figure 8) combined with that on the fiber structure.

In addition to the β_c relaxation, a broad E'' peak (or tan δ peak) was observed at ~25 °C (γ relaxation) and extended down to −150 °C. The E' decreased only slowly with increasing temperature in the range below 50 °C (Figure 5), and the ultradrawn fibers having a single-phase paracrystalline structure also exhibited this relaxation. These facts suggest that the γ relaxation is associated with local mode motions in paracrystalline phases. In contrast to the β_c relaxation at a higher temperature, the magnitude of the E'' and tan δ peaks

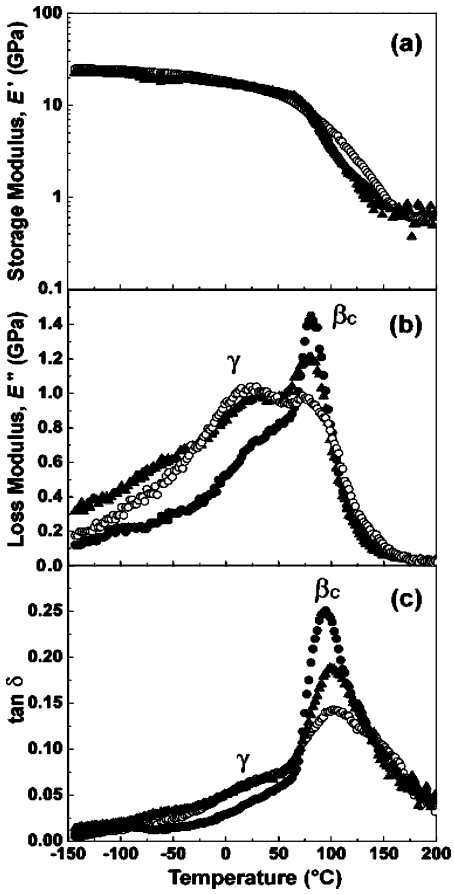

Figure 5. Dynamic storage modulus (E') (a), loss modulus (E'') (b), and loss tangent (tan δ) (c) vs temperature for a series of PAN fibers with an EDR of 16, measured in the draw direction at 3.5 Hz in the temperature range of −150−200 °C: (●) iso-PAN-3 fiber; (▼) iso-PAN-1 fiber; and (○) at-PAN fiber.

of the γ relaxation decreased with increasing isotacticity, suggesting that the syndiotactic and/or syndiotactic-rich sequences of PAN chains predominantly contribute to this γ relaxation. As discussed above, the WAXD study showed that these sequences take a planar zigzag chain conformation (Figure 3). It is also noted that although the ultradrawn iso-PAN-3 fiber with a DR_t of 60 showed only weak WAXD meridional scattering at around $2\theta = 36.3°$ (Figure 3), suggesting the existence of a small amount of planar zigzag sequences, this fiber also exhibited a weaker but clear E'' peak as a low-temperature shoulder of the β_c peak at 85 °C. Furthermore, the γ relaxation occurred through a wide temperature range (−150 to 50 °C) and associated with only a small decrease in the E'. These facts suggest that although this γ peak is primarily associated with the molecular motion of syndiotactic and/or syndiotactic-rich sequences, which take a planar zigzag chain conformation, the local mode motions of conformationally disordered sequences may also contribute to the γ relaxation.

Effect of Draw Ratio on the Relaxations. Figure 6 shows the E', E'', and tan δ for a draw ratio series of iso-PAN-3 with the highest isotacticity of 0.68. The gel film, which was brittle, was carefully fixed to the sample holders of a Rheovibron viscoelastometer. Nevertheless, it often broke upon cooling to low temperatures. Therefore, measurements on gel films were limited to the temperatures above −50 °C. The dynamic Young's modulus E' increased markedly with the DR_t in the whole range of temperatures studied, as shown in

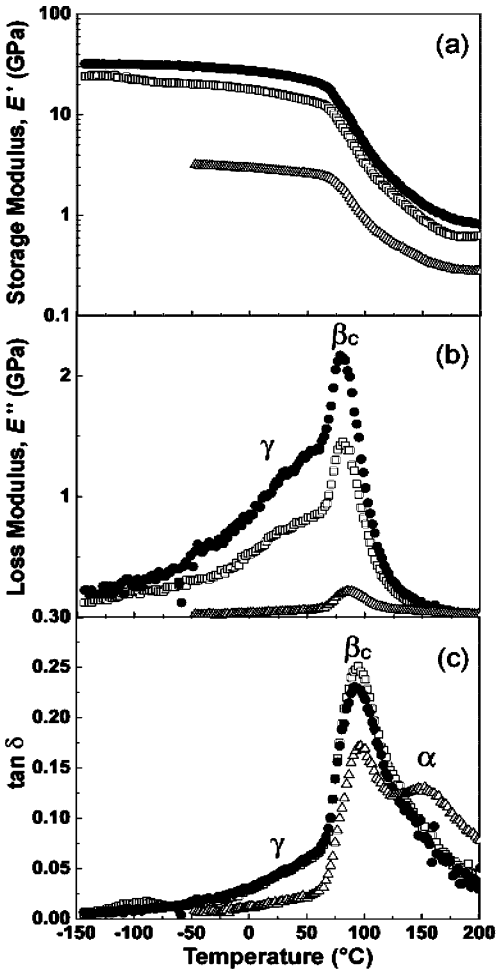

Figure 6. Dynamic storage modulus (E') (a), loss modulus (E'') (b), and loss tangent (tan δ) (c) vs temperature for a DR series of iso-PAN-3 with a $DR_t = 1-60$ measured in the draw direction at 3.5 Hz: (△) a gel film; (□) a fiber with an EDR of 16, and (●) a highly drawn fiber with a DR_t of 60.

Figure 6a. It decreased slowly up to ∼50 °C and then more rapidly with increasing temperature due to the onset of significant molecular motions. The drawn fibers show two E'' peaks (Figure 6b): a sharp peak at around 85 °C (β_c relaxation) and a broad one at around 25 °C (γ relaxation) observed as a shoulder of the sharp peak and extended down to −150 °C. The shapes and temperatures of these loss peaks were not significantly affected by the DR for the highly isotactic PAN. In addition to these two relaxations in drawn samples, the tan δ vs temperature curve of the gel film in Figure 6c clearly shows the existence of a tan δ peak at around 150 °C. The magnitude of this peak decreased upon drawing (Figure 6c) or annealing. Figure 7 shows three curves for an iso-PAN-3 gel film recorded by repeating the cyclic measurements from −50 to 200 °C. The tan δ curves in Figure 7c show that, although the shape and magnitude of the sharp tan δ peak at around 100 °C were not significantly affected, the magnitude of the tan δ peak at around 150 °C decreased significantly due to annealing when the measurements were repeated. These results confirm that this tan δ peak at around 150 °C is ascribed to the α relaxation associated with the molecular motion in disordered noncrystalline regions, as previously discussed on at-PAN.[18,21−23]

The relaxation behavior of at-PAN has been extensively studied.[13−23] However, the samples used in previ-

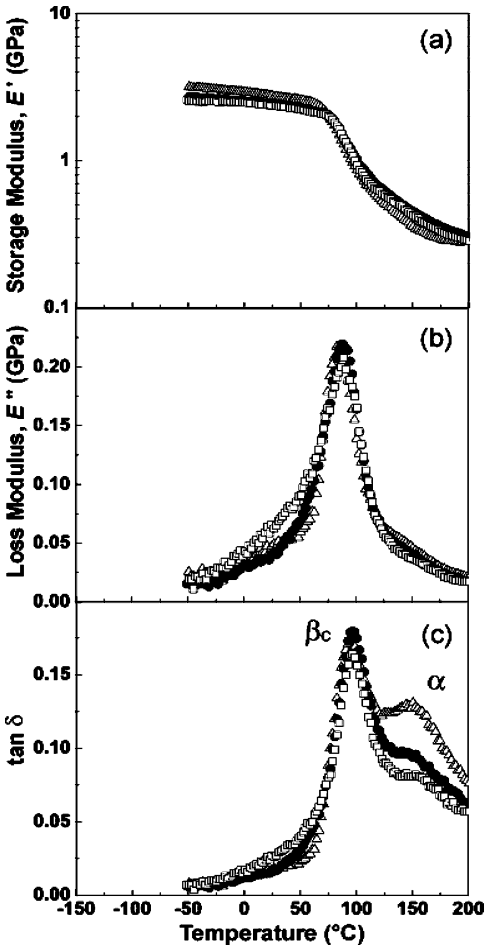

Figure 7. Dynamic storage modulus (E') (a), loss modulus (E'') (b), and loss tangent (tan δ) (c) vs temperature for a gel film of iso-PAN-3. The measurements from −50 up to 200 °C were repeated three times. Note that the magnitude of the tan δ peak decreased due to annealing when the measurements were repeated. (△) First, (●) second, and (□) third measurements.

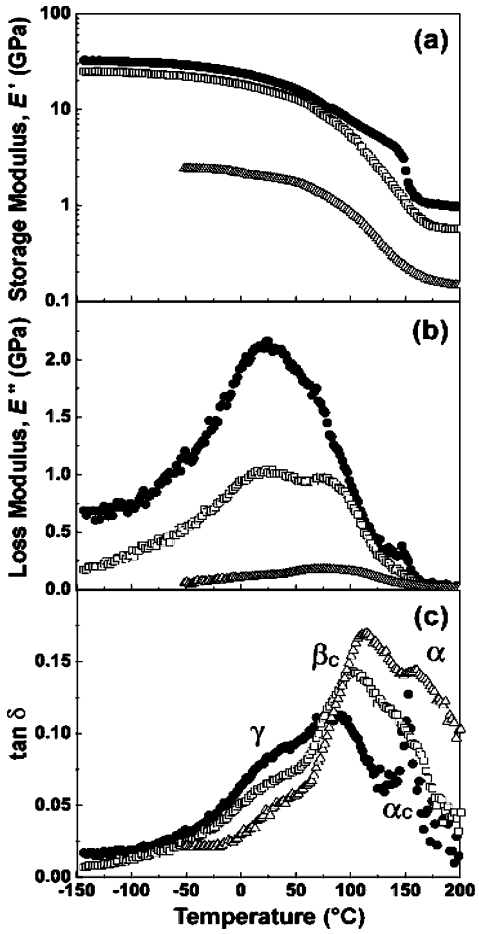

Figure 8. Dynamic storage modulus (E') (a), loss modulus (E'') (b), and loss tangent (tan δ) (c) vs temperature for a DR series of at-PAN fibers: (△) a gel film; (□) a fiber with an EDR of 16; (●) a highly drawn fiber with a DR_t of 60.

ous studies were limited to unoriented gel films and fibers with a low DR < 20. Figure 8 shows the E', E'', and tan δ as a function of the temperature for a series of drawn at-PAN fibers. Again, the measurements on gel films were limited to the temperatures above −50 °C. The data of an ultradrawn and extremely oriented (f_c = 0.996) at-PAN fiber with a DR_t of 60 are also included. Such an ultradrawn PAN fiber was not available until recently. The effect of DR_t on the dynamic mechanical behavior was more complex in at-PAN than in iso-PAN. Although the shapes of loss peaks and their temperatures were not significantly affected by the DR in iso-PAN, they were markedly affected by the DR in at-PAN, reflecting the conformational change upon drawing for at-PAN. In addition, an ultradrawn at-PAN fiber exhibited a sharp tan δ peak associated with a sharp drop in E' at around 150 °C that has different structural origin from the α relaxation that occurs at around 150 °C and is ascribed to the molecular motion in amorphous regions. To avoid confusion, thus, we will first discuss the α, β_c, and γ relaxations found in a gel film and a fiber with an EDR of 16 and then the unique relaxation in an ultradrawn fiber.

The tan δ vs temperature curves for a gel film of at-PAN measured at 3.5 Hz also exhibited a strong peak at around 100 °C and two weak peaks at around 150 and 25 °C that were associated with the β_c, α, and γ relaxations, respectively, as observed in an iso-PAN-3 gel film. The at-PAN fiber with an EDR of 16 also showed three relaxations at temperatures comparable to those found in the gel film. However, the magnitude and shape of the tan δ peaks were significantly altered upon drawing. The magnitude of the tan δ peaks due to the α (∼150 °C) and β_c relaxations (∼100 °C) decreased whereas that of the γ relaxation (∼25 °C) significantly increased upon drawing. The decrease in the magnitude of the tan δ peak due to the α relaxation upon drawing was caused by the increase in the crystallinity, as revealed by the density increase shown in Table 2.

However, both the decrease in the magnitude of the tan δ peak for the β_c relaxation and the increase in that for the γ relaxation upon drawing of at-PAN are related with the conformational changes in paracrystalline regions as observed by WAXD.[25] The meridional WAXD patterns of a draw ratio series of at-PAN revealed that the amount of helical sequences decreased and that of planar zigzag sequences increased upon drawing. Such effects of drawing on the relaxation behavior and chain conformation in paracrystalline regions of at-PAN are consistent with the assignment of the β_c relaxation to the molecular motion which was predominantly associated with helical sequences, as discussed above based on the effect of isotacticity on the magnitude of the tan δ peak for the β_c relaxation (Figure 5). In addition, the tan δ peak temperature for the β_c relaxation slightly shifted lower with increasing DR

Table 3. Activation Energies (kJ/mol) of the Relaxations for Various PAN Samples

	at-PAN			iso-PAN-3		
relaxation	gel film	EDR = 16	$DR_t = 60$	gel film	EDR = 16	$DR_t = 60$
α (150 °C)[a]	590 ± 100			580 ± 100		
β_c (100 °C)[a]	360 ± 20	290 ± 20		380 ± 20	385 ± 20	385 ± 20
γ (25 °C)[b]		63 ± 2	81 ± 2			

[a] tan δ peak temperature measured at 3.5 Hz. [b] E'' peak temperature measured at 3.5 Hz.

(Figure 8), reflecting the conformational changes upon drawing.

The γ relaxation observed as a broad E'' loss peak at around 25 °C and extended down to a low temperature of −150 °C was ascribed primarily to the local mode motions of syndiotactic and syndiotactic-rich, planar zigzag sequences because the magnitude of the E'' peak increased with decreasing isotacticity (Figure 5). Furthermore, at-PAN showed a significant increase in the magnitude of the tan δ peak due to the γ relaxation with increasing DR as shown in Figure 8, reflecting the increase of planar zigzag sequences with increasing DR.[25] The ultradrawn fiber with a DR of 60 had an extreme morphology, which was better approximated by a single-phase, paracrystalline structure in which a planar zigzag conformation was major (Figure 3a). This extreme fiber exhibited the strongest tan δ peak due to the γ relaxation, suggesting that this relaxation is primarily associated with the local mode motions of planar zigzag sequences in paracrystalline phases. It is noted, however, that the tan δ peak had a broad tail down to −150 °C. This suggests that the local mode motions of a wide variety of conformationally disordered sequences might be gradually initiated over the wide range of temperature and contributed to the lower temperature side of the γ relaxation.

Finally, the dynamic mechanical behavior of an ultradrawn at-PAN fiber with a DR_t of 60 is compared with those of a gel film and a drawn fiber with an EDR of 16. As shown in Figure 4, the ultradrawn fiber exhibited a DSC endothermic peak at 142 °C, which was ascribed to the first-order crystal/crystal transition from an orthorhombic to a hexagonal chain packing observed at around 150 °C by WAXD at elevated temperatures.[25] Corresponding to this transition, the E' decreased suddenly at 150 °C, the E'' showed a small peak, and the tan δ exhibited a sharp and strong peak at 150 °C (Figure 8). Thus, the relaxations at around 150 °C in at-PAN have two different origins due to the α and α_c relaxations depending on the DR. The former is associated with the micro-Brownian motion of disordered amorphous regions, which was clearly found in gel films of both the iso- and at-PANs. The latter is associated with the crystal/crystal first-order transition found only in ultradrawn at-PAN fibers with an extreme morphology showing high chain orientation ($f_c = 0.996$) and a high modulus approaching the still uncertain X-ray crystal modulus.[32] Furthermore, the amount of the planar zigzag sequences increased with increasing DR for at-PAN fibers.[25] Although the ultradrawn at-PAN fiber consists predominantly of highly oriented planar zigzag sequences, it still has a significant amount of helical sequences as shown by the scattering around $2\theta = 40°$ in the WAXD in Figure 3. These results, combined with a sharp drop in the dynamic modulus E' at 150 °C, suggest that this first-order transition may be associated with the molecular motion of planar zigzag sequences in the paracrystalline phases of ultradrawn at-PAN fibers with an extreme morphology. More details on this first-order transition are currently under investigation.

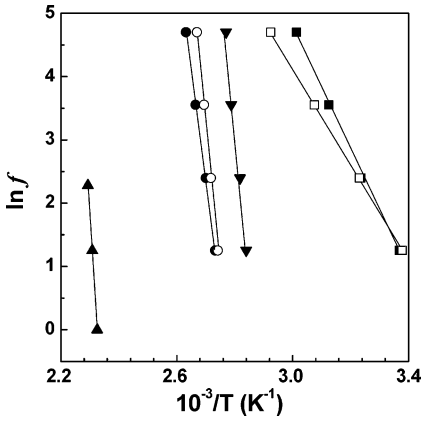

Figure 9. Plot of the logarithm of frequencies (ln *f*) against the reciprocal of tan δ peak temperatures ($1/T$). For the γ relaxation, the peak temperatures observed in E'' vs temperature curves were used since no clear tan δ peak corresponding to the γ relaxation was observed. α relaxation observed in a gel film for both iso- and at-PANs (▲), β_c relaxation in at-PAN with an EDR of 16 (●), in at-PAN gel film (○), and in iso-PAN with an EDR of 16 (▼); γ relaxations in at-PAN with an EDR of 16 (□) and in at-PAN with a DR of 60 (■).

Activation Energies for the Relaxations. To determine the effects of stereoregularity and DR on the activation energies for the α, β_c, and γ relaxations, the changes of the peak temperatures for tan δ and/or loss modulus E'' were measured as a function of the measurement frequency. Figure 9 shows the logarithm of frequency, ln *f*, plotted as a function of the reciprocal of the peak temperatures, $1/T$, in tan δ or E'' vs temperature curves measured for gel films, fibers with an EDR 16, and ultradrawn fibers of at-PAN and iso-PAN-3. The activation energies calculated from the slopes of these straight lines are summarized in Table 3. It is noted that the activation energies for the α and β_c relaxations in gel films of both iso- and at-PANs were 580−590 ± 100 kJ/mol and 360−380 ± 20 kJ/mol, respectively (Table 3). It is interesting to note that, although the activation energy for the β_c relaxation stayed constant for iso-PAN independently of the DR, that of at-PAN slightly decreased upon drawing reflecting the conformational change upon drawing. Although the activation energy for the γ relaxation in iso-PAN could be not determined because no clear loss peak was observed, the activation energy for at-PAN slightly decreased with increasing DR, reflecting the conformational change upon drawing.

Conclusion

The effects of stereoregularity and DR on the dynamic mechanical relaxations in PAN were studied for a series of well-characterized PAN's with ^{13}C NMR isotactic triad fractions ranging from 0.25 to 0.68 and drawn up to DRs of 60. Three relaxations of α, β_c, and γ were observed depending on the DR in both iso- and at-PANs

at around 150, 100, and 25 °C, respectively, as tan δ peaks measured at 3.5 Hz. In addition to these relaxations, α_c relaxation was observed at 150 °C only in an ultradrawn at-PAN. The shapes, magnitude, and temperatures of tan δ peaks and the activation energies of these relaxations were not significantly affected by the DR in iso-PAN, whereas they were markedly affected by the DR in at-PAN. These different effects of drawing on the relaxation behavior in iso- and at-PANs are ascribed to the fact the chain conformation of iso-PAN showed no significant change upon drawing, whereas that of at-PAN changed markedly upon drawing as found by WAXD. The characteristics of the four relaxations are summarized below.

The α relaxation was observed in gel films of both iso- and at-PANs and was ascribed to the micro-Brownian motion in amorphous regions, as previously reported. This relaxation was not significantly affected by the stereoregularity but diminished upon annealing or drawing due to the increase in the crystallinity.

The β_c relaxation was also observed in both iso- and at-PANs and was ascribed to the molecular motion in pracrystalline phases, as previously reported. However, it was found that the magnitude of the tan δ peak due to the β_c relaxation became larger with increasing isotacticity and hence helical sequences. Furthermore, the magnitude decreased upon drawing of at-PAN because the helical sequences decreased and the planar zigzag sequences increased upon drawing of at-PAN. These observations suggest that the β_c relaxation reflects predominantly the molecular motion of helical sequences in paracrystalline phases.

The γ relaxation was also observed in both iso- and at-PANs. However, the magnitude of the E'' or tan δ peak increased with decreasing isotacticity (Figure 5) and/or increasing DR in at-PAN (Figure 8). These facts suggest that this relaxation is mainly related with the local mode motions of syndiotactic and short isotactic sequences, which take a planar zigzag conformation in paracrystalline phases. The lower tail of this relaxation extended down to −150 °C is likely ascribed to the local mode motions of varieties of conformationally disordered segments.

Finally, the α_c relaxation that was observed at around 150 °C only in an ultradrawn at-PAN is associated with the molecular motion related with the first-order crystal/crystal transition. Although the observed effect of DR on the chain conformation in at-PAN suggests that this relaxation is likely associated with the molecular motion of the planar zigzag sequences (syndiotactic or short isotactic sequences), more details are currently under study.

Acknowledgment. This work was partly supported by a Grant-in-Aid from the Ministry of Education, Culture, Sports, Science, and Technology of Japan (#1550188). D.S. expresses his appreciation for the Sasakawa Scientific Research Grant from The Japan Science Society.

References and Notes

(1) Schmieder, K.; Walf, K. *Kolloid Z. Z. Polym.* **1953**, *134*, 149.
(2) Hinrichsen, G.; Orth, H. *Kolloid Z. Z. Polym.* **1971**, *247*, 844.
(3) Liu, X. D.; Ruland, W. *Macromolecules* **1993**, *23*, 3030.
(4) Stefani, R.; Chervreton, M.; Garnier, M.; Eyraud, C. *Comptes Rendues* **1960**, *251*, 2174.
(5) Kumamaru, F.; Kajiyama, T.; Takayanagi, M. *J. Cryst. Growth* **1980**, *48*, 2021.
(6) Bashir, Z. *J. Polym. Sci., Polym. Phys. Ed.* **1994**, *32*, 1115.
(7) Lindenmeyer, P. H.; Hosemann, R. *J. Appl. Phys.* **1963**, *34*, 42.
(8) Kaji, H.; Schmidt-Rohr, K. *Macromolecules* **2001**, *34*, 7368.
(9) Kaji, H.; Schmidt-Rohr, K. *Macromolecules* **2001**, *34*, 7382.
(10) Colvin, B. G.; Storr, P. *Eur. Polym. J.* **1973**, *10*, 337.
(11) Rizzo, P.; Auriemma, F.; Guerra, G.; Petraccone, V.; Corradini, P. *Macromolecules* **1996**, *29*, 8852.
(12) Kaji, H.; Schmidt-Rohr, K. *Macromolecules* **2000**, *33*, 5169.
(13) Howard, W. H. *J. Appl. Polym. Sci.* **1961**, *15*, 303.
(14) Bohn, C. R.; Schaefgen, J. R.; Statton, W. O. *J. Polym. Sci.* **1961**, *55*, 531.
(15) Kimmmel, R. M.; Andrews, R. D. *J. Appl. Phys.* **1965**, *36*, 3063.
(16) Hayakawa, R.; Nishi, T.; Arisawa, K.; Wada, Y. *J. Polym. Sci., Part A2* **1967**, *5*, 165.
(17) Okajima, S.; Ikeda, M.; Takeuchi, A. *J. Polym. Sci., Part A1* **1968**, *6*, 1925.
(18) Minami, S. *J. Polym. Sci., Appl. Polym. Symp.* **1974**, *25*, 145.
(19) Joh, Y. *J. Polym. Sci., Polym. Chem. Ed.* **1979**, *17*, 4051.
(20) Gupta, A. K.; Chand, N. *J. Polym. Sci., Polym. Phys. Ed.* **1980**, *18*, 1125.
(21) Cho, S. H.; Park, J. S.; Lee, W. S.; Chung, I. J. *Polym. Bull. (Berlin)* **1993**, *30*, 663.
(22) Rizzo, P.; Guerra, G.; Auriemma, F. *Macromolecules* **1996**, *29*, 1830.
(23) Bashir, Z. *J. Macromol. Sci., Phys.* **2001**, *B40*, 41.
(24) Yamane, A.; Sawai, D.; Kameda, T.; Kanamoto, T.; Ito, M.; Porter, R. S. *Macromolecules* **1997**, *30*, 4170.
(25) Sawai, D.; Yamane, A.; Takahashi, H.; Kanamoto, T.; Ito, M.; Porter, R. S. *J. Polym. Sci., Polym. Phys. Ed.* **1998**, *36*, 629.
(26) Holland, V. F.; Mitchell, S. B.; Hunter, W. L.; Lindenmeyer, P. H. *J. Polym. Sci.* **1962**, *62*, 145.
(27) Krigbaum, W. R.; Tokita, N. *J. Polym. Sci.* **1960**, *43*, 647.
(28) Sawai, D.; Kanamoto, T.; Porter, R. S. *Macromolecules* **1998**, *31*, 2010.
(29) Ogura, K.; Kawamura, S.; Sobue, H. *Macromolecules* **1971**, *4*, 80.
(30) Sawai, D.; Yamane, A.; Kameda, T.; Kanamoto, T.; Ito, M.; Yamazaki, H.; Hisatani, K. *Macromolecules* **1999**, *32*, 5622.
(31) Hu, X.; Johnson, D. J.; Tomka, J. G. *J. Text. Inst.* **1995**, *86*, 322.
(32) Allen, R. A.; Ward, I. M.; Bashir, Z. *Polymer* **1994**, *35*, 4035. They measured the variation of the X-ray *d*-spacings of the sharp equatorial reflections for an at-PAN fiber and determined the cross-sectional area of a chain as a function of the applied stress. By assuming that there was no volume change (i.e., Poisson's ratio $\mu = 0.5$) as the sample was strained, they estimated the strain along the chain axis of a crystal. Combining the stresses imposed on the fiber and the corresponding crystal strains, they constructed a stress/strain curve for an at-PAN crystal which gave an initial modulus value of 28 GPa along the chain axis.
(33) Kamide, K.; Ono, H.; Hisatani, K. *Polym. J.* **1992**, *24*, 917.
(34) Kamide, K.; Yamazaki, H.; Miyazaki, Y. *Polym. J.* **1986**, *18*, 819.
(35) Nakano, Y. PhD Thesis, Kanazawa University, 1995.
(36) Yamazaki, H.; Kajita, S.; Kamide, K. *Polym. J.* **1991**, *23*, 765.

MA0352330